INTERACTION BETWEEN CONCRETE AND SHEETING IN COMPOSITE SLABS

Milan Veljković, M.Sc. Doctoral Student

Luleå University of Technology, Division of the Steel Structures

S-971 87 LULEÅ

Telephone +46 920 72387
Fax. +46 920 91091
Milan.Veljkovic@anl.luth.se

ABSTRACT

The purpose of this paper is to give insight into the mechanical interlocking mechanism and into the behavior of composite slabs based on numerical analysis. Small scale push tests and friction tests are used to obtain interaction properties between sheeting and concrete. The focus is on the distribution of slip and longitudinal shear stresses between concrete and sheeting, the distribution of longitudinal strains in the sheeting and in the cross section. It is assumed that the shear connection in a composite slab can not function unless there is slip at the interface between concrete and the sheeting. The general range of validity of small scale tests and the potential for improvement of partial connection strength methods are laid out.

Key words: Partial interaction, Small scale test, Nonlinear finite element analysis, 3D model, Mechanical model

1. INTRODUCTION

Composite floors consisting of a concrete deck and a thin-walled steel sheeting can be used as a competitive floor design in construction. The flooring deck system has been in use since the early 1950s in the USA and is common in multistory steel framed buildings.

Composite floors have a great variety of applications in the construction industry (office and industrial buildings, carpark units, renovation schemes) and they can be used in conjunction with concrete or timber structures as well. Lightweight concrete is commonly used instead of normal weight concrete in order to reduce the self weight, in the United Kingdom for example.

The sheeting has two roles. During the casting of the concrete it serves as a formwork and after the concrete has hardened it serves as reinforcement.

In the seventies composite slabs were considered as structural elements similar to reinforced beams. Consequently, the design methods for longitudinal shear and vertical shear are based on empirical methods similar to those used for reinforced beams. The m-k method is still a broadly accepted method for longitudinal shear design in USA /1/ and in European national codes, as well as in Eurocode 4 /2/.

At the end of the eighties, composite slabs began to be considered as structural elements similar to composite beams. The partial connection strength method, derived primarily for composite beams / 3/, /4/, has been suggested as an appropriate method for the design of composite slabs failing in longitudinal shear. Currently, two variants of the partial connection method exist. One, which is proposed in Eurocode 4 /2/, was developed by J.B.W. Stark and H.Bode together with their collaborators, and one that was developed by Patrik 1994 /5/. The importance of friction developed at the support between sheeting and concrete was first recognized by Patrik 1990 /6/.

In this paper results from tests and finite element modeling carried out at Luleå University of Technology /7/, /8/ will be presented.

2. ULTIMATE LIMIT STATES OF A COMPOSITE SLAB

The design of composite floors in Eurocode 4 /2/ and Swedish code /9/ is based on experimental results obtained for simply supported composite slabs loaded with two line loads. Three failure modes can be defined as follows:

(a) *Longitudinal shear failure* occurs if the shear span (corresponding to the development length in reinforced concrete) is not sufficiently long to ensure the transfer of the force from the concrete deck to the steel sheeting which is required for a plastic moment in the composite slab. The concrete then slips over the sheeting at a load which is less than the load which causes flexural resistance $M_{p.R}$ of the slab calculated according to elastic-rigid plastic theory using an effective sheeting area.

(b) If the flexural capacity of a slab (defined with respect to an effective sheeting area) is reached, then the composite slab can be considered to fail in a *flexural failure* mode. In this case the interaction properties of the sheeting, namely the strength and ductility of the mechanical interlocking devices, do not limit the flexural capacity. The presence of the mechanical interlocking devices, e.g. indentations, reduce the sheeting area. The effective sheeting area is a supplementary information obtained after full scale testing, /7/. It should be noted that at the ultimate state, the concrete deck slips over the sheeting. This is a consequence of large strains in sheeting, which are a few times larger than the yield strains. The strain level is dependent on the shear span and the slenderness of the slab. In the codes /2/, /9/, /10/ complete interaction between concrete and sheeting is assumed for this failure mode.

(c) *Vertical shear failure* occurs across the width of the span when the transverse shear capacity of the concrete deck is reached. An important characteristic of vertical shear failure is that the ultimate load is not limited by the longitudinal shear capacity of the slab and, of course, is smaller than the load which causes flexural failure. It has been shown in /5/ and /11/, and /12/ that the vertical shear provisions of Eurocode 4 are conservative when used to design Bondek II and Plannja Combideck, respectively.

3. LONGITUDINAL SHEAR TRANSFER

3.1 General

Sheeting profiles, with respect to their performance in composite slabs, can be divided into two groups. The first group suffers *brittle longitudinal shear failure* while the second group develops *ductile longitudinal shear failure*. The behavior of composite slabs is defined as ductile /2/ if the failure load exceeds the load causing first recorded end slip by more than 10%. The total load at which the end slip is 0.5mm is accepted in /7/ as the load corresponding to "first recorded end slip" and is compared with the failure load. The issue of ductility of composite slabs should in fact be related to the ductility of the mechanical interlocking resistance, which is a relation between the horizontal force (shear stress) and the slip measured in the small scale pusb test. The amount of slip for which the maximum horizontal force needs to be kept constant in order to ensure ductile behavior for a certain slab, is currently studied at LuTH.

Various sbeeting profiles with different types of indentations are shown in /13/. For plain, reentrant sheeting additional end anchorages are required /14/. The role of the sheeting profile, especially the reentrant portion is important. The reentrant portion is ideal for resisting vertical separation /15/. The optimization of the sheeting profile can be done with the small scale push test as shown in /7/.

The *interaction* between profiled sheeting and concrete, after the adhesion is broken, is ensured by mechanical interlocking, and possibly also by frictional locking and friction at the support:

- *Mechanical interlocking action* is produced by the indentations pressed into the web (the most common case), or by small dents pressed into the apex of the fold along the bottom flange, (as e.g. in sheeting profile Peva 45). In general, the mechanical interlocking characteristics (slip secant modulus, ductility, maximum transfer force from the concrete to the sheeting) depend on the type of the indentations or embossments, and their size and position on the sheeting profile.

- *Frictional locking produced along the rib* is caused by the reentrant portion of the sheeting profile. It is not necessary to separate the contributions of frictional locking and mechanical interlocking measured in the small scale push test, see /7/ for example.

- *Friction produced at the support* is caused by the reaction force and has to be treated separately.

Adhesion between concrete and sbeeting exists but is often neglected because of its brittle nature and unreliable strength (large scattering of the measured shear capacity).

M.Patrik has found that the strength of the concrete has a certain influence on the longitudinal shear strength /5/.

The load-slip relationship measured in small scale tests characterizes the functions of composite slab and is similar to the bond-stress-slip relationship for reinforced bars measured in pull-out tests. Upon comparing results from pull-out tests performed on reinforced bars at LuTH /16/ with results of small scale push tests /7/, the interaction properties between concrete and sheeting or reinforcement appear to be remarkably similar regarding the shapes of the curves. However, a large difference appears in the resistance.

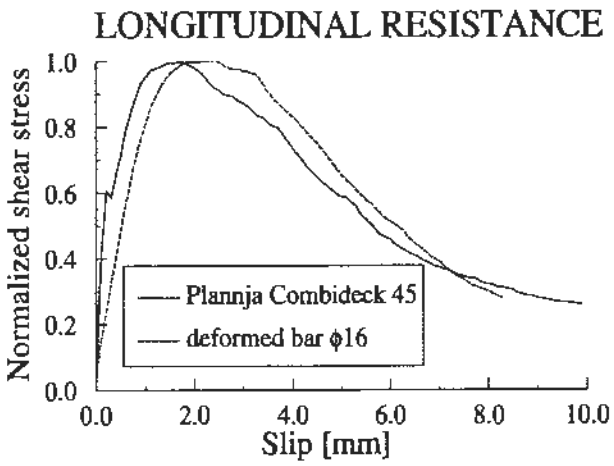

Figure 1. Comparison of push test for sheeting /6/ and the pull-out test of reinforcement /16/, /17/

The maximum bond stress for a reinforcement bar depends on the bar diameter and the concrete density. For example, the maximum bond stress of a deformed bar Φ16 with f_{yk}=380MPa and normal strength concrete (NSC) with f_{cc}=47MPa is 19.3 MPa /17/, while the longitudinal shear resistance calculated with the projected sheeting area of Plannja Combideck 45 is 0.41 MPa. The shear resistance of the reinforced bar and the sheeting profile, shown in Figure 1, is normalized with respect to the maximum value obtained.

Some characteristics of the interaction performance of various sheeting profiles are presented in /5/, /18/, /19/, /20/, /21/ and in this paper, while the main references related to the mechanics of shear transfer with reinforcement can be found in /21/, /16/.

3.2 Mechanics of the interaction between sheeting and concrete

In order to understand the behavior of composite slabs it is important to know the way in which the tensile force occurring in the sheeting is transferred to the surrounding concrete. Mechanical locking and frictional locking are two contributors to the longitudinal shear resistance that might be qualitatively identified in an example using the sheeting profile Plannja Combideck 45. In the push test the total horizontal force is measured.

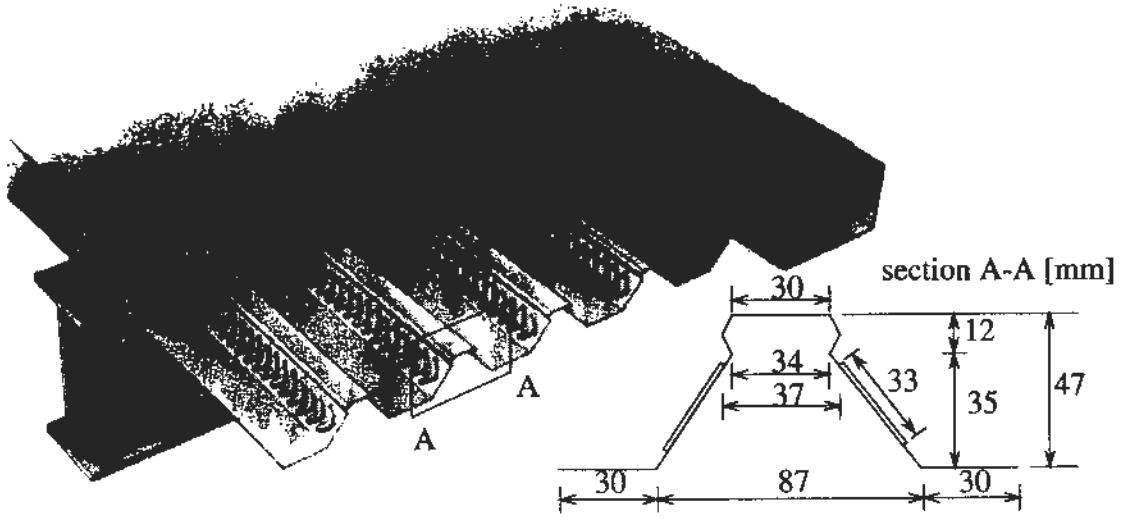

Figure 2. Plannja Combideck composite floor, courtesy of Plannja AB Luleå

The mechanics of the interaction between sheeting and concrete during the overriding of the concrete over the sheeting are the same both in the small scale push test as well as in the composite slab. A possible equilibrium state is shown in Figure 3. The ends of the indentations, *position 1*, are the main contributors to mechanical interlocking. The *mechanical interlocking forces*, defined as forces produced by the presence of indentations which act as obstacles to the overriding of the concrete over the indentations, can be split into *two components*. The first component, which is in the longitudinal direction, contributes to the measured *horizontal force* in the push test. The second component, which is assumed to act perpendicular to the web, is considered in the model as an *action on the sheeting*. The bending of the webs, due to overriding of the concrete block over the indentations, causes bending of the flanges in the opposite direction. The concrete however restrains the flanges' bending. Compressive vertical forces arise at the contacts between the concrete and the flanges, which tend to lift the concrete from the sheeting. The position of the vertical forces on the concrete, *position 2*, depends on the sheeting profile, and on the direction and distribution of actions on the web. If the simplified actions are assumed to be perpendicular to the web and have the same intensity for both forces at *position 1*, then lifting force acts only at the bottom flange. There is no contact between concrete and sheeting at the top flange. Therefore possible forces are indicated with gray arrows in Figure 3.

The force at *position 3* together with the frictional forces which arise because of the slip between concrete and sheeting in the plane of the cross section maintain equilibrium with the discretized action on the sheeting. The force at position 3 can be named the *splitting force* because its counter part acting on the concrete has a tendency to split the concrete. The magnitude and direction of the splitting force, which arises in the small scale push test and in the composite slab away from the support, is dependent on the shape of the reentrant portion, the indentations' characteristics (depth, position on the web, pitch distance and volume), and the sheeting thickness. The splitting force can be so large that it causes splitting of the concrete which originates at the peak of the reentrant portion. Splitting failure is more likely to occur with a lightweight concrete, as is the case in the push test /7/ and in the composite slab /23/.

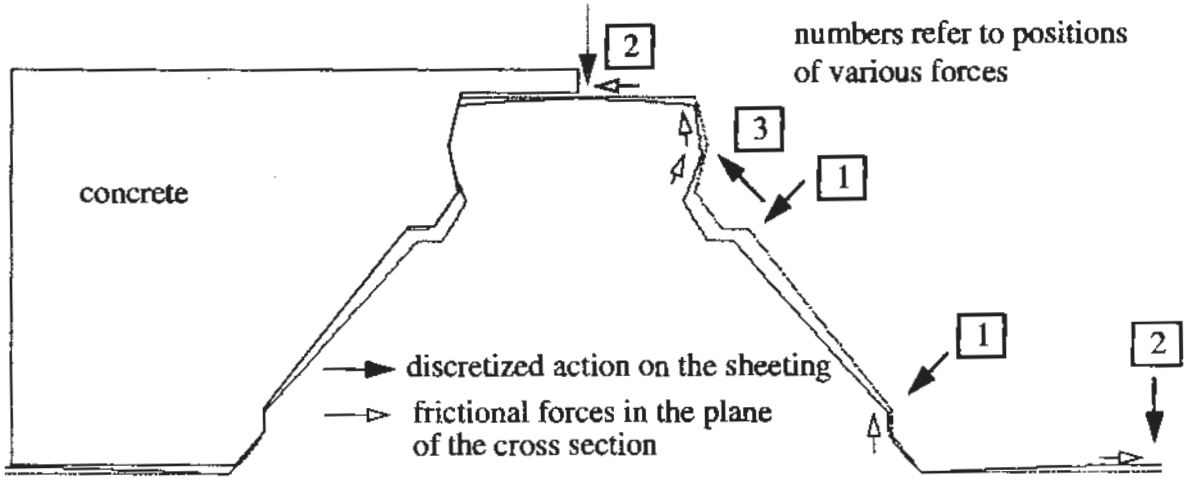

Figure 3. Bending of sheeting during concrete overriding. The original and the deformed shape of the sheeting are shown.

The *frictional locking force* which arises primarily at *position 3* acts parallel to the rib. The magnitude of this force is linearly related to the splitting force by the friction coefficient. Of course, wherever the concrete and the sheeting are in contact, at *position 1* as well, frictional (locking) forces arise in the direction of the slip. Furthermore, at *position 2* frictional forces of low magnitude arise.

The relation between the horizontal force and the slip measured in the push test is called the mechanical interlocking resistance because: *firstly*, it is desirable that the major contribution to the horizontal force is caused by the mechanical interlocking (many sheeting profiles tested /7/, /18/, /19/, /20/, /21/ have only this type of the shear transfer), and *secondly*, the frictional locking can not appear alone in the small scale test /7/ but only as a consequence of mechanical locking e.g. bending of the sheeting as shown in Figure 3.

4. FINITE ELEMENT MODEL OF THE COMPOSITE SLAB

4.1 General

In the following examples, the finite element system DIANA Version 5.1 has been used to model two line load bending tests of composite slabs with 2.0 and 4.0 m spans, respectively. Both slabs extend 100 mm beyond the centre of the support. Due to symmetry, only one sixteenth of the composite slab is modelled. Two 0.8 mm thick plates, known as crack inducers, which follow the sheeting profile in a perpendicular direction, were positioned under the applied load in order to better define the shear span during the test.

4.2 Sheeting

The trapezoidal shape of the sheeting is modelled with curved shell elements. Measured data for a characteristic rib, Figure 2, is approximated for the numerical model and shown in Figure 6. Based on tensile tests of dimpled and flat sheets, different uniaxial stress-strain relationships are used for the web and flanges. A dimpled sheet is that part of the web which has indentations. Test results obtained for specimens containing only dimpled sheet were used to derive the effective material of the web with a "two bar model" /7/. The effect of the cold forming on the sheeting properties (yield strength and ductility) is not considered.

The pressed indentations reduce the effective yield stress and Young modulus to 47% of the original values for a flat sheet, see Figure 4. This is a consequence of the flexural deformations of the folds that are added to the extensional deformation. A plasticity model with von Mises yield surface and isotropic hardening is used. The assumption that the sheeting material is isotropic is not fully correct and isotropic hardening is not correct for the general case, but this assumption does not lead to a large deviation from the actual behavior of the slab since uniaxial tension is the dominating stress in the sheeting.

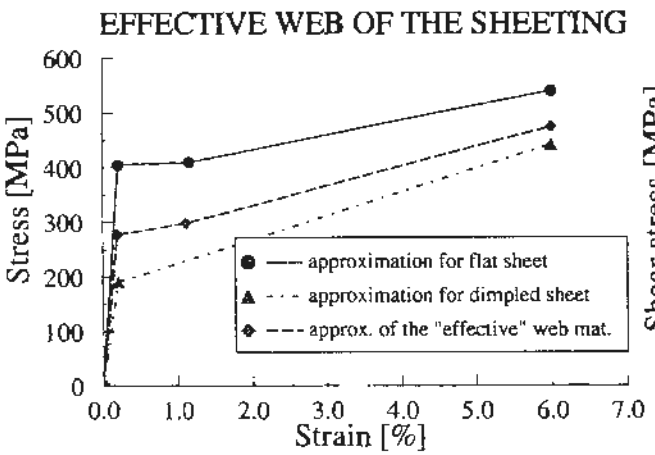

Figure 4. Sheeting material

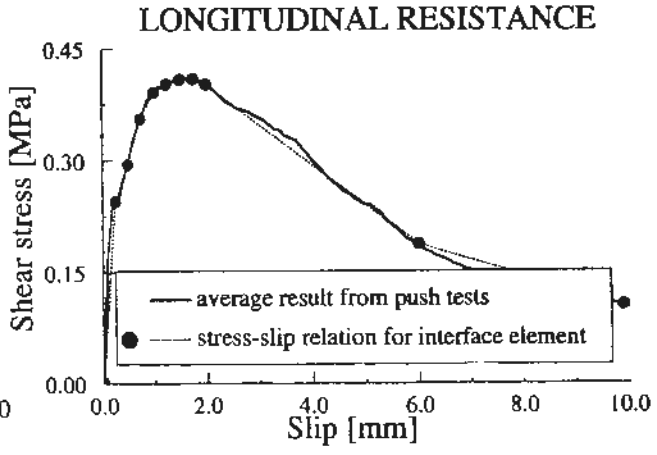

Figure 5. Sheeting shear stress-slip diagram

4.3 Sheeting-concrete interaction properties

4.3.1 Mechanical interlocking

Longitudinal shear resistance produced by the indentations and by the re-entrant portion at the contact between sheeting and concrete is modelled using a nodal interface element called N4IF. A non-linear elastic constitutive model is used for the longitudinal slip-stress relation. The constitutive model is appropriate until substantial reverse slip occurs. Results from a small scale push test provide the basis for this relation, Figure 5. The force-slip relationship measured in the test is simply mapped onto a stress-displacement curve by dividing the forces by the developed area of the approximated sheeting.

The nodal interface elements are placed at the corners of the shell elements and connected to the solid elements. The allocation of the shear transfer to the interface elements has almost no influence on the composite slab behavior described by the load-displacement diagram.

In order to compensate for the overhang at the support, the first interface element which transfers horizontal shear caused by mechanical interlocking has an allocated area which is 2.5 times larger than that of the adjacent element in the longitudinal direction.

Sheeting-concrete interface properties are assumed to be independent of the strain level in the sheeting. This assumption causes the capacity and ductility of composite slabs which fail in flexure to be overestimated. The decrease of interface properties due to the high strain level in the sheeting is, however, not yet known.

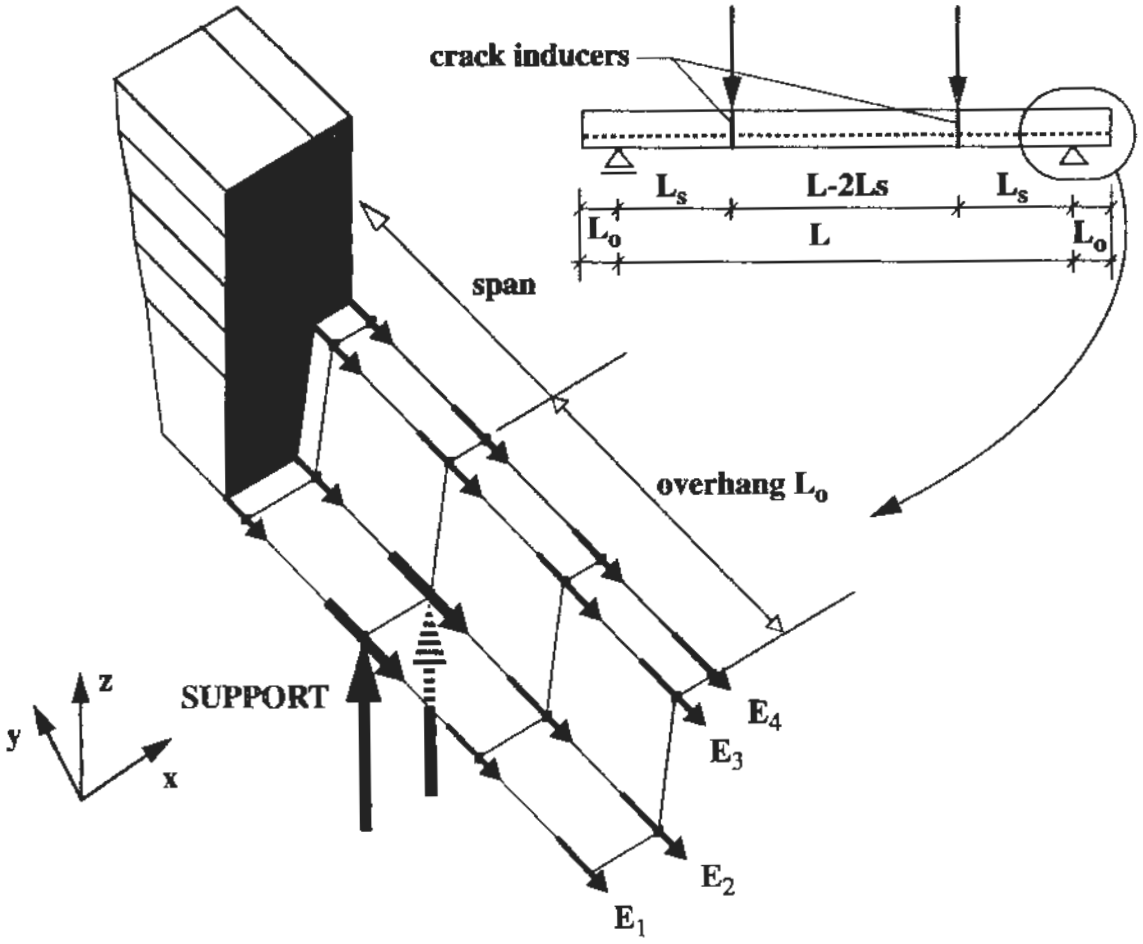

Figure 6. Model of the longitudinal interaction between sheeting and concrete

In the vertical direction, linear elastic behavior with two different stiffnesses is assnmed. A very large elastic modnlus is used for the outer interface elements, lines E_1 and E_4 in Figure 6, causing vertical separation between sheeting and concrete deck to be prevented at all times. An almost negligible elastic stiffness is assigned to the springs at the folds, E_2 and E_3. In this way the shear force in the web is underestimated. The vertical spring stiffness is not derived from tests (some doubt exists as to if it is possible to derive). It is believed that this stiffness is not important if the vertical separation is effectively prevented by the profile. The vertical separation between sheeting and concrete leads to a redncti on of horizontal shear transfer which is considered in an assumed relation between horizontal shear and slip, Figure 5.

4.3.2 Friction

The sheeting is supported only at the bottom flange i.e. at two of the nodes in lines E_1 and E_2.

Friction at the support is modelled with a nodal interface element for which the Coulomh friction criterion is used. The friction coefficient of 0.6 was obtained from friction tests /7/. It is assumed that the surfaces of the concrete and the sheeting neither react chemically (no adhesion) nor dilate (the surfaces are perfectly smooth); therefore, both the cohesion and the dilatancy angle are chosen to be zero.

The frictional slip condition (yield condition) $\tau = \mu\sigma$ and the strain increment $d\vec{\varepsilon} = (d\varepsilon, d\gamma) = (0, d\gamma)$ assumed in the model are shown in Figure 7. It is obvious that because the dilatancy angle is zero, the normality condition is not satisfied. For a detailed description of the frictional continuum see /24/, /25/.

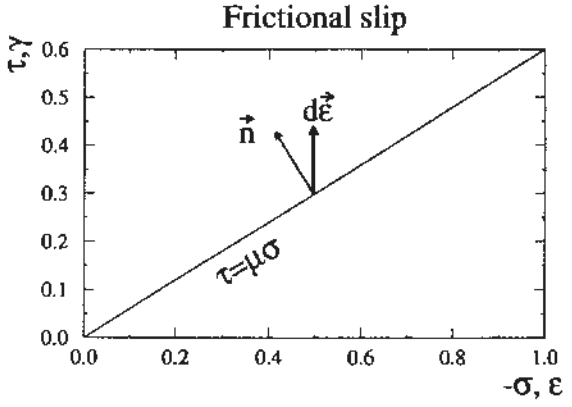

Figure 7. Coulomb yield criterion

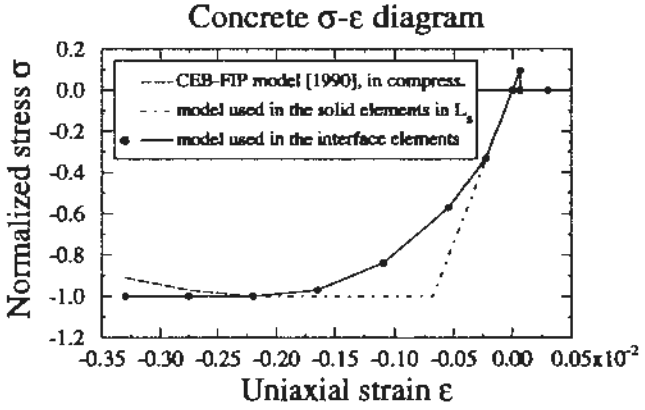

Figure 8. Basic uniaxial σ--ε relation for concrete

4.4 Concrete

The concrete deck is modelled with solid elements in the shear span, and solid elements and plane interface elements in the region of constant bending moment. An elastic material with a Young modulus for concrete is assigned to the solid elements in the region of constant bending moment. The length of the solid elements is 50 mm which corresponds to the average distance between the flexural cracks recorded during the experiments with the 4m span composite slab. This mesh is too coarse to allow the introduction of interface elements into the shear span in order to use predictor-corrector technic /26/. Thus, in the shear span, the cracking of the concrete is modelled using only the smeared approach. In the region of the constant bending moment, characterized by flexural cracks,

the interface elements are placed between each column of solid elements. A nonlinear elastic constitutive model based on the material properties of concrete is used. This is chosen to ensure nonlinearity of the concrete in compression, according to CEB-FIP model 1993 /27/, since it is well known that concrete behaves in a highly nonlinear manner in the ascending region of uniaxial compression, see for example /28/. The consequence of this approach is that the transfer of vertical shear is the same in both the cracked and uncracked concrete. This is not seen as a limitation of the model. This is because only vertical cracks (fracture mode I) have to be modelled since no vertical shear exists in the region of constant bending moment. Thus, a constant value for the shear modulus is used with a large dummy modulus in the plane of interface. The length of the solid elements, 50 mm, is used as a base length in order to calculate the relative displacement normal to the crack.

The smeared approach is used to describe cracking of the concrete in the solid elements. The plasticity model used for compression has a Drucker-Prager description of the yield surface. The shear retention factor β=0.20 is used for numerical convenience, since it was found to be more suitable in the considered case than β=0.0 usually recommended for reinforced beams. This choice is not compatible with the description of the concrete in interface elements hut, as will be shown in the numerical examples, this is not a decisive factor in the analysis.

4.5 Crack Inducers

A quadrilateral interface element is used to model the crack inducer, which in a numerical sense means that the strains are concentrated in the discrete crack. A nonlinear elastic constitutive model based on the material properties of the concrete is used, hut since no adhesion between the crack inducer and the surrounding concrete is assumed, the arbitrary value 0.1 MPa is assigned as the tensile strength and brittle cracking is used. The length of the solid elements, 50mm, is used as the base length in calculating the relative displacement normal to the crack.

5. COMPARISON OF EXPERIMENTAL AND NUMERICAL RESULTS

5.1 General

The experimental results (applied load and midspan displacement) were corrected for the self weight of the slab and the weight of the test set-up. The displacement due to the self weight was calculated with the moment of inertia for an uncracked slab and assuming full interaction between concrete and sheeting. The concentrated forces that caused the same midspan displacement as the displacement calculated from the gravity loads were summed and the actuator force corresponding to gravity load was obtained. This force and the midspan displacement were added to the measured actuator force and the average midspan displacement, respectively.

The average midspan displacement was calculated from data obtained from two LVDTs placed on the upper surface in the middle of the slab.

The test curves and the numerical results are normalized with respect to the load causing the plastic bending moment in the slab. The full sheeting area (nominal sheeting area) is used in normalizing the experimental and numerical results and in calculating the plastic moment capacity. In Figure 9 and 10 a comparison between the experimental results and numerical predictions is shown for slabs which failed in longitudinal shear and flexure, respectively.

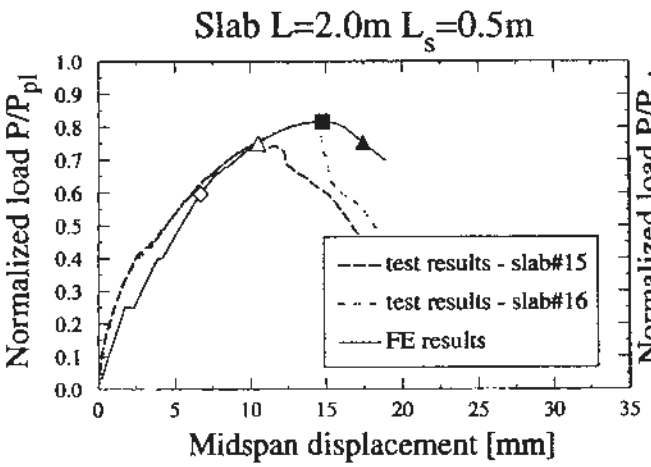

Figure 9. Load-displacement diagram for slab failing in longitudinal shear

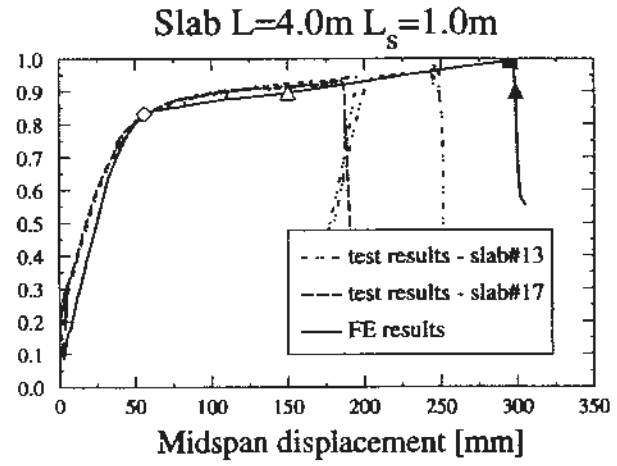

Figure 10. Load-displacement diagram for slab failing in flexure

Load-midspan displacement results from two tests are compared with the numerical results. It is shown in /7/ that the reason for the lower capacity of slab #15 is an error in the specimen's design. The specimen was designed with insufficient constraints on the sideways bending of the longitudinal sides of the sheeting. The result obtained for slab #16 is comparable with the numerical simulation, but not with the descending branch of the curve. The sudden drop in bearing capacity after the maximum load is reached is due to insufficient constraints on the sidways bending of the longitudinal sides of the slab.

At the early stages of loading the numerical calculations for both spans predict larger deformation than it was obtained in the experimental results. There are three reasons for this:
- The constraint effect of the concrete on the accordion effect of the dimpled sheet is neglected. This gives a Young modulus which is too small for the effective web material. The difference between the actual modulus and the Young modulus used in the calculation is greatest at the beginning of the numerical simulation.
- The adhesion between concrete and sheeting is completely neglected in the numerical simulation because this effect has a brittle nature and because a large scattering of the measured adhesive strength was obtained in the small scale push tests. However, adhesive stresses are active at the beginning of the full scale tests, which ensures full interaction between concrete and sheeting, and also gives the crack inducer some tensile strength.
- The concrete is given zero fracture energy for numerical convenience. It was shown in /8/ that different descending branches of concrete in tension do not give qualitatively new information which is of importance for understanding the two considered failure modes, but reduce the discrepancy between the experimental and numerical results only at the lower load levels.

There are two important reasons for differences between numerical results obtained in /8/ and here. The first is that the implementation of nonlinear concrete behavior in the compression region makes the slab more flexible. Therefore, the load-displacement curve calculated herein lies under that of experimental results. The second, which is especially important for the 4 m span slab, is that an expected reduction of the mechanical interlocking due to the presence of large strains in the sheeting is taken into account in a more realistic way than in /8/. This results in a higher ultimate load, see Figure 10. The mechanical interlocking resistance of the interface elements in a region 500 mm long, between 500 mm and 1000 mm from the support, is reduced to 50% of the resistance obtained from the push tests. This part of the sheeting, which is in the shear span, has strains larger than the yield strain at the maximum load.

Note that certain load (displacement) levels on the numerical load-displacement curves, in Figures 9 and 10, are emphasized by symbols which are used in the following diagrams showing the specific characteristics at the corresponding levels.

5.2 Longitudinal slip between the concrete and sheeting

The concrete deck slides over the sheeting in the shear span from the very beginning of loading because of the longitudinal shear stress-slip relation (mechanical interlocking) assigned to the interface elements, see Figure 5. The maximum slip occurs under the applied load and decreases toward the support. This tendency is the same for any shear span length, see Figure 11, but the difference in appearance of the slip distribution is influenced by the ductility of the mechanical interlocking. Longer shear spans have steeper slip gradients close to the position of applied load. In this region, the longitudinal shear stress-slip relation is on the descending branch due to the large crack width while the measured load is still increasing.

The end slip (slip at the end of slabs) at maximum load for the longer spans is never higher than for shorter spans. If this does not hold true it might indicate a mistake in the specimen's preparation, for example, unsatisfactorily prevented sideways bending of the longitudinal edges of the sheeting [7]. The predicted end slip at the maximum load for both slabs closely agrees with the experimental results. The measured end slip (distance from the support is 0 in Figure 10.) for slabs #16 (L=2.0 m) and slab#13 (L=4.0 m) was 1.5 mm and 1.0 mm respectively.

In both slabs the concrete deck finally slides over the sheeting in the shear span, but at a very different mobilized horizontal force, see Figure 11. The slab fails by longitudinal slip if the axial force in the sheeting is not sufficient to cause yielding in the entire cross section of the sheeting. Such a failure mode represents the governing bearing capacity for shorter slabs, in the following example, slabs with 2.0m and 0.5 m shear spans.

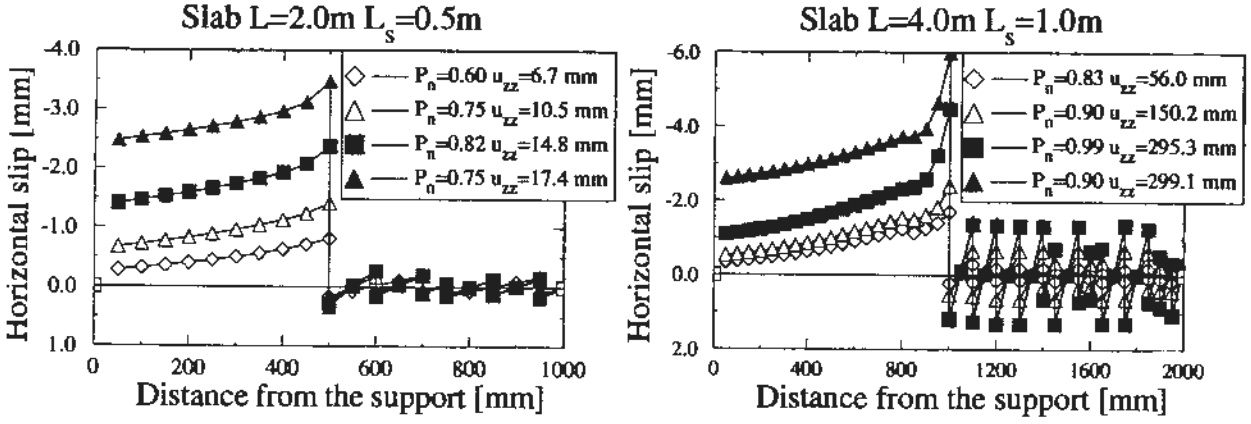

Figure 11. Slip between the concrete deck and the sheeting at different load levels

5.3 Distribution of longitudinal shear stress

A very important insight into the longitudinal shear stress distribution is obtained from the model. An almost uniform distribution of the maximum shear stresses in the shear span is achieved, Figure 12, where the longitudinal interface stress is normalized with its maximum value. If the contributions

of the friction at the support and the mechanical interlocking resistance in the shear span are considered separately /8/, then the shear capacity measured in the push test is nearly reached. The specimen used in the push test consisted of a concrete block cast on one 250 mm long sheeting rib. The small difference between measured shear capacity and average shear stress produced by mechanical interlocking in the slab is the result of the mechanical interlocking ductility, for slip larger than 1.75mm the longitudinal shear resistance of the sheeting deteriorates.

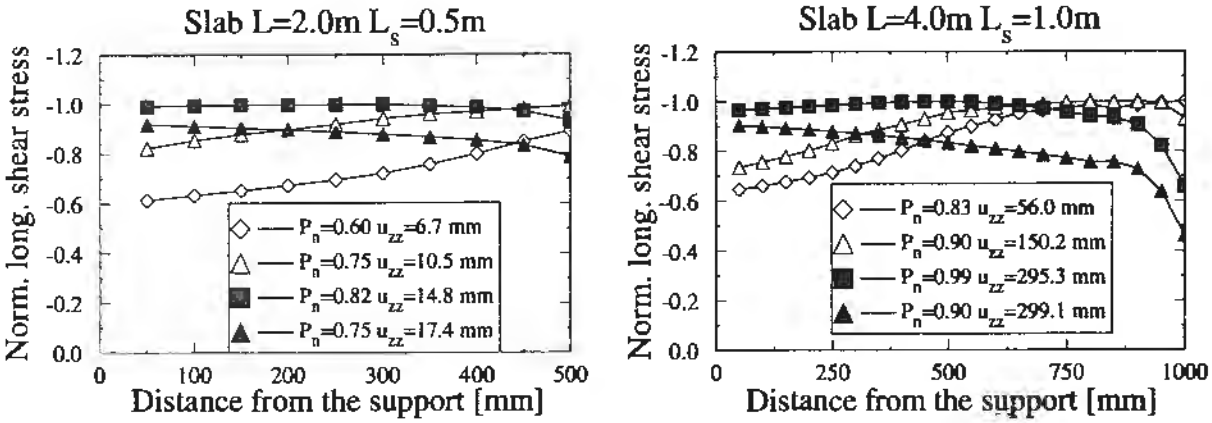

Figure 12. Longitudinal shear stress distribution at the bottom flange in the shear spans for slabs failing in longitudinal shear and flexure

5.4 Cumulative force in the interface elements

The mobilized longitudinal force for the slab depends on the sheeting's shear resistance (mechanical interlocking capacity and ductility), the friction between sheeting and concrete that appears at the support, and the shear span length. The cumulative force is the sum of all the horizontal forces between the support and the cross section in question, which includes the frictional forces at the support and the mechanical interlocking forces in the shear span. A contribution of the mechanical interlocking resistance activated on the overhang to the cumulative force is shown 50mm from the support. At that position, the first interface element with the nonlinear constitutive relation which models the mechanical interlocking resistance is placed.

The cumulative force increases in the shear span and is constant in the region of constant bending moment as shown in Figure 13. The stress resultant in the sheeting is equal to the cumulative force, and, of course, to the compressive force in the concrete at the considered cross section.

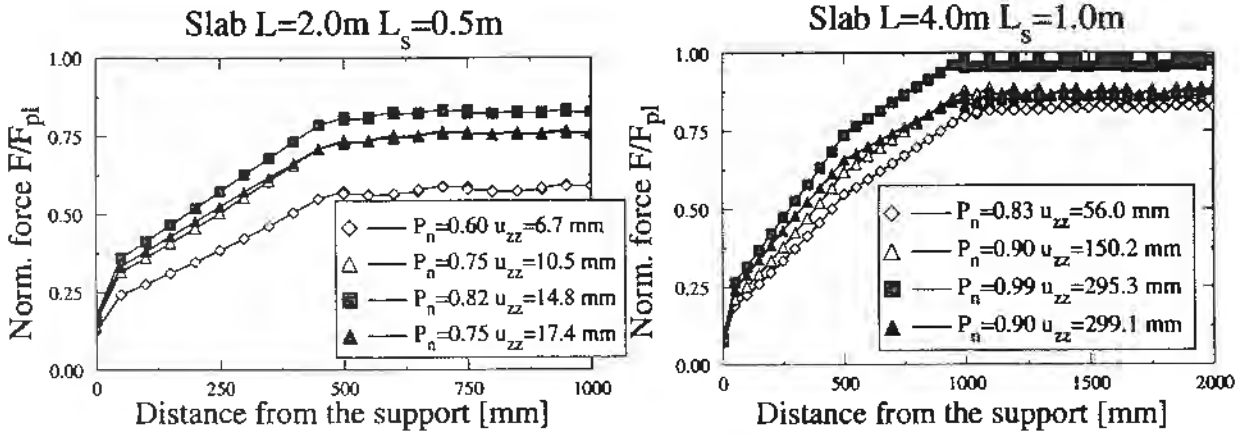

Figure 13. Cumulative force in the sheeting at the maximum load

Note that sudden change in the gradient of the cumulative force at 500mm from the support for the slab L=4m is due to assumed reduction of the mechanical interlocking capacity because of large strains in the sheeting.

5.5 Normal strain in the sheeting and concrete

As an indication of the strain status of the sheeting, an average value of the longitudinal strains ε_{yy} in the bottom and top flanges and in the web are calculated from two values obtained at the integration points in the cross section. The integration points are located at the bottom of the shell element. The strains in the sheeting are not only dependent on the slab curvature but also on the intensity of the longitudinal forces transferred by the interface elements from the concrete deck to the sheeting. The greater influence of the friction introduced at the bottom flange at the support is obvious for the shorter spans because of the larger reaction force. The cracking of the concrete causes redistribution of internal strains so that under the cracked concrete the sheeting is locally bent. Because of the two model assumptions, first that no uniform load is considered and second that the concrete has zero fracture energy, several small cracks appear in the region of constant bending moment. This was approximately correct for the longer span where small cracks were fully opened in the experiment, so that the distribution of the strains would be very close to the numerical prediction. In the case of the shorter span two major cracks appeared, one under the applied load and another in the midspan, therefore slightly higher strains in the midspan then numerically predicted could be expected in the experiment.

The diagrams in Figure 14 show that all of the sheeting is in tension. It might be possible however to have the upper flange in compression for a deep sheeting profile.

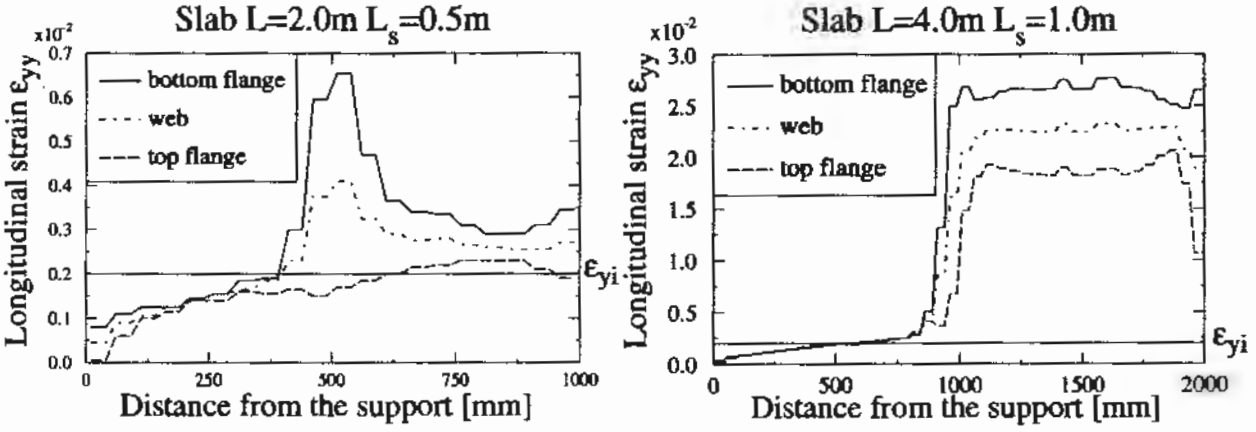

Figure 14. Strain distribution in the sheeting at maximum load

6. CONCLUSIONS

1. The mechanics of the force transfer from the sheeting to the concrete at the slip is qualitatively analyzed. The same governing mechanism is found in both the small scale push test and the full scale test. The parameters measured in the small scale push test (horizontal force and slip relation) and the friction test (friction between concrete and sheeting) are sufficient to predict the behavior of composite slabs which fail in longitudinal shear.

2. Three parameters are important for the interaction between sheeting and concrete:

- longitudinal shear resistance of the sheeting caused by mechanical interlocking
- friction between sheeting and concrete at the support
- reduction of the longitudinal shear resistance of the sheeting due to large strains in the sheeting

These three parameters are needed to completely describe the interaction properties of composite slabs and to extend the application of small scale test results to composite slabs which fail in flexure.

3. Uniaxial tests of dimpled sheet and flat sheet provide data for a safe evaluation of sheeting performance. The accordion effect in dimpled sheet /7/ is important for bending resistance and for deformation. The effective web material concept of the sheeting is found suitable for FE implementation.

4. Close agreement between the experimental load-displacement curve and the FE prediction is obtained for longitudinal shear failure. The differences obtained for slabs which fail in flexure indicate a need to experimentally establish the reduction of longitudinal shear resistance of the sheeting due to large strains in the sheeting.

ACKNOWLEDGMENTS

Financial support of this work has been provided by The Swedish Council for Building Research.
The writer would like to thank Prof. Bernt Johansson, Div.of Steel Structures, for his valuable guidance and many stimulating discussions. Mr. Valle Janssen has read the english text and his comments has been very valuable. The experimental work was performed in the TEST-lab at Luleå University of Technology.
Acknowledgment is due to Plannja AB, Luleå for releasing test data for publication.

NOTATION

u_{zz}	vertical midspan displacement of the slab [mm]
F	force [N]
F_{pl}	force calculated according to rigid plastic theory [N]
L	slab span [m]
L_s	shear span [m]
$M_{p.R}$	maximum flexural resistance of the slab calculated with effective sheeting are according to rigid plastic theory
$P_n = P/P_{pl}$	normalized concentrated force
P	total concentrated force on the composite slab [N]
P_{pl}	concentrated force on the slab causing the fully plastic bending moment accord ing to rigid plastic theory in the slab calculated with the nominal sheeting area [N]
ε	normal strain
$d\varepsilon$	normal strain increment
$d\vec{\varepsilon}$	strain vector increment
ε_{bottom}	normal strain in the longitudinal direction of the slab at the bottom flange at the elastic limit

ε_{yy}	normal strain in the longitudinal direction of the slab
ε_{yi}	yield strain
γ	shear strain
$d\gamma$	shear strain increment
μ	friction coefficient
σ	normal stress [MPa]
τ	shear stress [MPa]
τ_{xy}	shear stress at the interface between concrete and sheeting [MPa]

REFERENCES

/1/ W.Samuel Easterling Craig S. Young: Strength of Composite Slab, Journal of Structural Engineering. Vol.118, No 9, 1992, pp. 2370-2389.

/2/ Eurocode 4, ENV 1994-1-1:1993, Design of Composite Steel and Concrete Structures.

/3/ R.P.Johnson and I.M.May, Partial-interaction Design of Composite Beam, The Structural Engineer No 53, August 1975, pp. 305-311.

/4/ R.P.Johnson: Loss of Interaction in Short-span Composite Beams and Plates, Journal of Constructional Steel Research, Vol.1, No 2, January 1981, pp. 11-16.

/5/ M. Patrik: Shear Connection Performance of Profiled Steel Sheeting in Composite Slabs, 2 volums, Doctoral Thesis presented at School of Civil and Mining Engineering, The University of Sydney, February, 1994.

/6/ Patrik M.: A New Partial Shear Connection Strength Model for Composite Slabs, Steel Construction J., Australian Institute of Steel Construction, Vol.24, Num 3, 1990, pp. 2-17.

/7/ M. Veljkovic: Development of a new sheeting profile for composite floors, Experimental study and interpretation, Tulea 1993:47, Luleå University of Technology, Luleå 1993, Sweden.

/8/ M.Veljkovic: 3D Nonlinear Analysis of Composite slabs, G.M.A. Kusters and M.A.N Hendriks (eds.) DIANA Computational Mechanics '94, Kluwer Academic Publisher, The Netherlands, pp. 395-404.

/9/ Swedish Regulations for Steel Structures BSK, English translation published by Swedish Institute of Steel Structures, Publication 118, Stockholm 1989, pp. 183.

/10/ BS5950: Part 4, Code of Practice for Design of Floors with Profiled Steel Sheeting, British Standard Institution, 1982.

/ 11/ M.Patrik and R.Q. Bridge: Design of Composite Slabs for Vertical Shear, Composite Construction in Steel and Concrete II: Proceedings of an Engineering Foundation Conference (eds. W.S Easterling and W.K.M.Roddis) pp. 304-322.

/12/ M. Veljkovic: Composite slabs, Proc. of Eurocode 4 Seminarium 15-16 sept. 1994, Swedish Institute of Steel Construction, ed. L.Hamrebjörk, pp.107-128, (in print).

/13/ M. Crisinel: Composite slabs, IABSE Short Course Brussels 1990, Notes, Volume 61, pp. 67-87.

/14/ H.Bode, R.Künzel, J.Schanzenbach: Profiled Steel Sheeting and Composite Action, Ninth International Speciality Conference on Cold Formed Steel Structures, St.Louis, Missouri, USA 1988, pp.343-359.

/15/ H.R.Evans, H.D.Wright: Steel-concrete composite flooring deck structures, Steel-concrete composite structures, ed. by R.Narayanan, Elsevier Applied Science Publishers, London 1988, England, pp.21-52.

/16/ K.Noghabai, Splitting of Concrete in the Anchoring Zone of Deformed Bar - a Fracture Mechanics Approach, licentiate thesis, Luleå University of Technology, Luleå Sweden, (to be published 1995).

/17/ K. Noghabai, U. Ohlsson, T. Olofsson, Bond Properties of High Strength Concrete, Proc. of Symposium Utilization of High Strength Concrete, June 20-23 1993 Lillehammer, Norway, eds. I. Holand and E. Sellevold, pp.1109-1176.

/18/ B. Daniels: Shear Bond Pull-out Tests for Cold-formed-steel Composite slabs, Publication ICOM 194, Jun 1988.

/19/ J.B. Daniels, M.Crisinel: Composite Slab Behaviour and Strength Analysis, Part I: Calculation Procedure, Part II Comparisons with Test Results and Parametric Analysis, Journal of Structural Engineering. Vol.119, No 1, 1993, pp. 1-49.

/20/ K.C.Jolly, A.K.M.Zubair : The Efficiency of Shear-Bond Interlock Between Profiled Steel Sheeting and Concrete, Proc. of Int.Conf. on Steel and Aluminium Structures, Composite Steel Structures-Advance, Design and Construction, ed. Narayanan R., Cardif, 1987, pp.127-136.

/21/ An Li.: Load Bearing Capacity and Behaviour of Composite Slabs with Profiled Steel Sheet, Doctoral Thesis, Chalmers University of Technology, Göteborg, 1993.

/22/ C.v.d. Veen: Cryogenic Bond Stress-Slip Relationship, Doctoral Thesis, Delft University of Technologu 1990.

/23/ C.T.Duffy, D. O'Leary: Shear Bond Capacity Tests on Composite Slabs with Combideck, Maj 1994, Private property of Plannja AB Luleå.

/24/ Z. Bazant: Advanced Topics in Inelasticity and Failure of Concrete, Swedish Cement and Concrete Research Institute, 1979.

/25/ Z. Bazant, L.Cedolin: Stability of Structures; Elastic,Inealastic, Fracture, and Demage Theories, Oxford Engineering Science Series, Oxford University Press, 1991.

/26/ J.G.Rots: Computational Modeling of the Concrete Fracture, Doctoral Thesis, Delft Univ. of Technology, 1988.

/27/ CEB-FIP Model Code, Comite Euro-International du Beton, Lausanne, Maj 1993.

/28/ W.F.Chen, D.J.Han: Plasticity for Structural Engineers, Springer-Verlag, 1988.